

Cite this: DOI: 10.1039/c2cs35272a

www.rsc.org/csr

## REVIEW ARTICLE

## Complexes of earth-abundant metals for catalytic electrochemical hydrogen generation under aqueous conditions†

V. Sara Thoi,<sup>ab</sup> Yujie Sun,<sup>ab</sup> Jeffrey R. Long<sup>\*ac</sup> and Christopher J. Chang<sup>\*abd</sup>

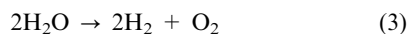
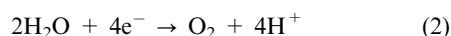
Received 20th July 2012

DOI: 10.1039/c2cs35272a

Growing global energy demands and climate change motivate the development of new renewable energy technologies. In this context, water splitting using sustainable energy sources has emerged as an attractive process for carbon-neutral fuel cycles. A key scientific challenge to achieving this overall goal is the invention of new catalysts for the reductive and oxidative conversions of water to hydrogen and oxygen, respectively. This review article will highlight progress in molecular electrochemical approaches for catalytic reduction of protons to hydrogen, focusing on complexes of earth-abundant metals that can function in pure aqueous or mixed aqueous–organic media. The use of water as a reaction medium has dual benefits of maintaining high substrate concentration as well as minimizing the environmental impact from organic additives and by-products.

## 1. Introduction

Climate change and rising global energy demands have prompted an urgent search for new renewable energy solutions. While great technological advances in accessing sustainable forms of energy such as wind and solar power have been made, the storage of these energies for on-demand usage and transport remains a major challenge. Molecular fuels offer an attractive option for resolving this issue owing to the high energy density that can be concentrated within chemical bonds.<sup>1–3</sup> In particular, the splitting of water into hydrogen and oxygen in separate half reactions is a promising path forward as this process is completely carbon neutral as shown in the following equations:



Ideally, water splitting can be driven by sustainable energy sources such as solar and wind power, and the sole combustion product from burning hydrogen is water. With the eventual goal of incorporating both half reactions in an integrated artificial device driven by a sustainable energy input, an essential scientific

challenge to address is the design and implementation of efficient catalyst systems for water reduction and oxidation.

Focusing on the reductive side, the catalytic conversion of protons to hydrogen (reaction (1)) is the key fuel-generating transformation for water-splitting cycles. Nature provides exquisite examples of catalysts in the form of hydrogenases, which are capable of using earth-abundant iron and/or nickel metal centers to reversibly interconvert protons to hydrogen at low thermodynamic potentials with high efficiencies and activities (rates up to 100–10 000 moles of hydrogen per mole of catalyst per second).<sup>4–6</sup> Notable advances in utilizing hydrogenases for water splitting applications have been reported and their catalytic mechanisms can be studied in molecular detail.<sup>4,7–11</sup> However, challenges remain in utilizing these complex macromolecules, including the low density of metal active sites compared to their overall large size and their relative long-term instability under ambient conditions.<sup>11–15</sup> On the other hand, heterogeneous catalysts based on platinum and other precious metals are much more robust, but suffer from high cost and low abundance.<sup>16–19</sup> As such, alternative extended solids based on more earth-abundant elements, including mixed metal alloys,<sup>3</sup> molybdenum-based heteropolyacids,<sup>20–22</sup> and molybdenum sulfide,<sup>23–27</sup> are being actively explored. However, heterogeneous systems by definition are more difficult to study as their performances are highly dependent on local variations in surface morphology and chemical reactivity.

Against this backdrop, an indispensable scientific bridge between the areas of homogeneous biological and heterogeneous solid-state catalysts is small-molecule chemical systems. Indeed, well-defined synthetic catalysts for proton reduction are valuable in many respects as they can (i) offer opportunities to fine-tune their performance and study their catalytic mechanism at a molecular level, (ii) provide discrete models for complex biological

<sup>a</sup> Department of Chemistry, University of California, Berkeley, California 94720, USA

<sup>b</sup> Chemical Sciences Division, Lawrence Berkeley National Laboratory, Berkeley, California 94720, USA

<sup>c</sup> Materials Sciences Division, Lawrence Berkeley National Laboratory, Berkeley, California 94720, USA. E-mail: jrlong@berkeley.edu

<sup>d</sup> Howard Hughes Medical Institute University of California, Berkeley, California 94720, USA. E-mail: chrischang@berkeley.edu

† Part of the solar fuels themed issue.

or extended materials, and (iii) serve as lead compounds to identify new motifs capable of hydrogen production under a variety of conditions. In particular, electrochemical methods have become a convenient route to probe these catalytic systems as well as use them as test beds for future integration into artificial devices. In this review, we will summarize progress in small-molecule approaches to electrocatalytic hydrogen evolution, focusing on systems that are compatible with aqueous media.

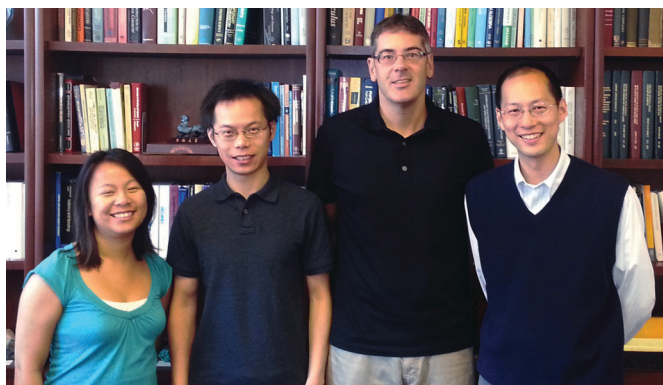
### 1.1 Scope of the review

Water splitting and catalytic hydrogen production are expansive and important topics and have been the subjects of several recent reviews.<sup>3,28–30</sup> To distinguish this article from those published previously, we will confine our discussion in the following three ways. First, we will focus on exclusively electrochemical studies using well-defined small-molecule electrocatalysts, noting that biological and extended materials offer complementary approaches to proton reduction. Second, we will restrict our discussion to systems that utilize only earth-abundant metal centers that can be readily extracted and refined from the earth's crust, which is in line with long-term sustainability issues of cost and scalability. Finally, we will highlight catalysts that can operate in either pure aqueous or mixed aqueous–organic solutions. The use of water as both a green solvent and a substrate for hydrogen generation offers the dual benefits of maintaining high substrate concentrations as well as minimizing

environmental impacts from organic additives and by-products. Although the ultimate goal for electrocatalytic proton reduction is to use water as both the solvent and the substrate, most proton reduction catalysts to date operate only in non-aqueous media with organic additives. We hope to bridge this gap with mixed aqueous–organic systems to demonstrate efforts toward complete water compatibility.

### 1.2 Metrics for evaluation of electrocatalytic systems

Growing interest in electrocatalytic systems for hydrogen production continues to provide a rich and ever-expanding library of new catalytic motifs for study. At the same time, the diverse array of operating conditions for these systems, including variations in the proton source, electrolyte, solvent, and working electrode, often makes direct comparisons of catalytic activity, efficiency, and stability challenging. One common complication is the use of different electrochemical references in the literature, which is a central issue for comparing catalytic systems operating under mixed solvents, as the reference potential can differ greatly depending on the solvent conditions. Although we acknowledge that such corrections have inherent limitations, for the sake of simplicity, we have adopted a standardized conversion between Ag/AgCl, SCE, or Fc/Fc<sup>+</sup> to SHE for evaluating the range of catalysts reported to date. These corrections are as follows: Ag/AgCl (water), +0.210 V; SCE (water), +0.240 V; Fc/Fc<sup>+</sup> (acetonitrile, water–acetonitrile), +0.640 V.



**V. Sara Thoi, Yujie Sun, Jeffrey R. Long and Christopher J. Chang**

*V. Sara Thoi received a BS degree in chemistry from the University of California, San Diego, and graduated with honors in 2008. She received the Mayer Award for Excellence in Undergraduate Research for her work on coordination chemistry of novel metal dipyrin complexes in the laboratory of Prof. Seth M. Cohen. She is currently a graduate student in the laboratory of Prof. Chris Chang at UC Berkeley, and was awarded a NSF Graduate Research Fellowship in 2009. Her general interests lie in green chemistry and sustainable energy research, with an emphasis on catalytic water splitting and carbon dioxide reduction.*

*Yujie Sun received a BS degree with honors in 2005 from Fudan University, China, working with Prof. Heyong He as a Chun-Tsung scholar. Thereafter, he pursued graduate studies at Ohio State University with Prof. Claudia Turro, focusing on ruthenium and osmium polypyridyl complexes as luminescence sensors and photodynamic therapy agents. After earning his*

*PhD in 2010, Yujie moved to postdoctoral studies with Prof. Chris Chang at UC Berkeley. His current research interests lie in the field of renewable energy catalysis, with a particular interest on molecular and solid-state catalysts for electro- and photochemical water splitting.*

*Jeffrey R. Long received a BA degree from Cornell University in 1991 and earned his PhD from Harvard University in 1995. He is currently a Professor of Chemistry at the University of California, Berkeley, and a Faculty Senior Scientist in the Materials Sciences Division at Lawrence Berkeley National Laboratory. In addition, he is the lead-PI for the Berkeley Hydrogen Storage Program, Deputy Director of the Berkeley Center for Gas Separations Relevant to Clean Energy Technologies, and a founding Associate Editor for Chemical Science. With over 150 publications, his research areas include the synthesis of inorganic clusters and solids with unusual electronic and magnetic properties, generation of microporous metal–organic frameworks for applications in gas storage, separations, and catalysis, and the development of molecular catalysts for electro- and photochemical water splitting.*

*Christopher J. Chang is an Associate Professor of Chemistry and a HHMI Investigator at UC Berkeley. He received his BS and MS degrees from Caltech in 1997, working with Prof. Harry Gray. After a year as a Fulbright scholar in Strasbourg, France, with Dr Jean-Pierre Sauvage, Chris received his PhD from MIT in 2002 under the supervision of Prof. Dan Nocera. He stayed at MIT as a postdoctoral fellow with Prof. Steve Lippard and then began his independent career at UC Berkeley in 2004. Research at the Chang lab is focused on chemical biology and inorganic chemistry, with particular interests in molecular imaging and catalysis applied to neuroscience, stem cells, cancer, infectious diseases, renewable energy, and green chemistry.*

In addition, the nature of an acid in mixed aqueous–organic media should be addressed as the thermodynamic potential of reducing protons is a function of the  $pK_a$  of the proton source.<sup>31</sup> The  $pK_a$  of an organic acid in non-aqueous solvent may vary dramatically depending on the concentration of water, particularly for weak acids ( $pK_a > 20$ ).<sup>32,33</sup> Acids with conjugate bases that have highly localized negative charge are better solvated by water, and this phenomenon can increase their acidity in organic media.<sup>32,33</sup> Unfortunately, the effect on  $pK_a$  for solutions containing more than trace ( $> 1\%$ ) amounts of water has not been well-studied. Thus, caution must be exercised in direct comparisons of the activity of catalysts in different media.

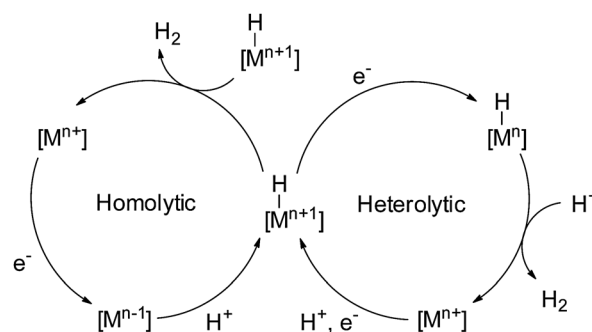
For clarity, we define here a list of terms typically used to assess and compare electrocatalytic activity. Overpotential ( $\eta$ ) is defined as the standard reduction potential of the  $H^+/H_2$  couple under the operating conditions subtracted from the applied potential ( $\eta = E_{\text{applied}} - E$ ) and represents the driving force needed to reduce protons to  $H_2$  beyond the thermodynamic potential. Methods on how to determine overpotentials have been a subject of discussion in several previous reports,<sup>31,34</sup> but for the purpose of this review we will only cite the overpotential reported in the literature. Faradaic efficiency or Faradaic yield is the ratio of moles of  $H_2$  generated divided by half the charge (expressed in Faraday units) passed in a controlled potential electrolysis, and represents the efficiency of a catalyst to consume charge and put it towards productive hydrogen evolution chemistry. The turnover number (TON) is the total number of moles of  $H_2$  generated per mole of catalyst from a controlled potential electrolysis and is often used to assess the overall stability of a catalyst. The turnover frequency (TOF) is defined as the TON per unit of time and is a kinetic parameter; this value can be extracted from the amount of charge passed in a controlled potential electrolysis in a given time or from digital simulation if the mechanism is known. Alternatively, the observed rate constant,  $k_{\text{obs}}$ , can be used as a proxy for TOF under pseudo-first order conditions in acid where there is negligible consumption of protons and can be calculated from cyclic voltammetry measurements using the following equation:<sup>35</sup>

$$\frac{i_c}{i_p} = \frac{n}{0.4463} \sqrt{\frac{RTk_{\text{obs}}}{F\nu}} \quad (4)$$

Here,  $i_p$  is the peak current of the catalytic potential in the absence of acid,  $i_c$  is the catalytic peak current plateau,  $n$  is the number of electrons involved in each catalytic turnover,  $R$  is the universal gas constant ( $8.314 \text{ J K}^{-1} \text{ mol}^{-1}$ ),  $T$  is the temperature (K),  $F$  is the Faraday constant ( $96485 \text{ A s mol}^{-1}$ ), and  $\nu$  is the scan rate.

### 1.3 Mechanistic and design principles for effective hydrogen production catalysts

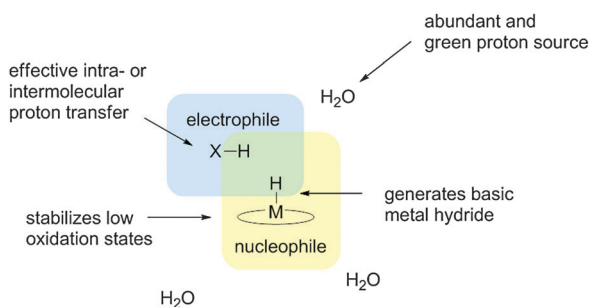
Careful consideration of the various potential mechanistic pathways for proton reduction is important for designing effective hydrogen production catalysts. Mechanistic studies of electrocatalytic  $H_2$  generation by molecular metal precursors, including Co complexes in particular, have been investigated both experimentally and theoretically.<sup>36–41</sup> In most cases,  $H_2$  evolution



**Scheme 1** Proposed mechanisms for  $H_2$  evolution *via* the formation of a common metal-hydride intermediate. Note that the M designation is generalized and can represent monometallic or multimetallic hydrides, as well as metal-hydrides with non-innocent ancillary ligands to provide additional redox equivalents.

is thought to proceed through a common metal-hydride intermediate, formed by either consecutive or coupled proton and electron transfers, and is followed by two possible pathways for subsequent H–H bond formation (Scheme 1). We note that, for simplicity, these generic structures are depicted as monometallic hydrides, but that multimetallic hydrides as well as metal-hydrides with high metal–ligand cooperativity *via* non-innocent ligands are also reasonable starting points. The first path involves a homolytic mechanism, where two metal-hydride complexes generate  $H_2$  *via* reductive elimination. Alternatively, a heterolytic pathway can occur, where the metal-hydride complex is further reduced and protonated to evolve  $H_2$ . In this latter case, two electrons and two protons are delivered to a single metal center and a putative  $H-[M^n]$  is formed, suggesting that the  $H-M^{n+1}/H-M^n$  couple plays an important kinetic role in the H–H coupling process. Distinguishing between homolytic and heterolytic mechanisms is often challenging, as both pathways may simultaneously occur or interconvert depending on the pH or acid strength of the given system.<sup>42</sup> In addition to the formation of metal-hydride complexes,  $H_2$  generation can also be facilitated through protonation of an external donor that resides in the first- or second-coordination sphere. For example, nitrogen amines, as well as sulfur and oxygen donors, have been exploited as protonation sites, particularly for sterically-congested metal complexes.<sup>43–46</sup> These systems operate as frustrated Lewis pairs, in much the same way as the natural hydrogenase systems utilize pendant redox-active cofactors or second-sphere amines to actively control proton delivery to a nucleophilic, reducing metal core.

Taken together, these mechanistic considerations highlight several design criteria that need to be met for creating effective catalytic systems for producing hydrogen from water. First and foremost, metal catalysts should have available open coordination sites and the appropriate electronic characteristics for generating a basic metal-hydride species (Scheme 2). As noted above, single-metal and multimetallic sites can be equally successful in this regard. Second, a ligand platform that can stabilize reducing metal species should be chosen to minimize the electrochemical overpotential needed for proton reduction. Such redox tuning can be achieved primarily at the metal core or *via* metal–ligand cooperativity using non-innocent redox-active ligands. Alternatively, systems where available protonation sites can



**Scheme 2** Design parameters for an effective proton reduction catalyst that operates through a generic metal-hydride intermediate.

be integrated into the superstructure offer another approach for tuning overpotential. Indeed, in natural hydrogenases, the tertiary structure of proteins plays a crucial role in their reactivity by controlling both proton and electron inventories. Using these same principles for artificial systems, building an appropriate secondary coordination sphere surrounding a metal-based active site, such as installing basic groups like amines<sup>47</sup> and oximes,<sup>36</sup> may assist in intra- and intermolecular proton transfer and thus enhance catalytic activity. In all cases, the use of water as a solvent offers the patent benefit of maintaining high local substrate concentration. With these criteria in mind, the remainder of this review will highlight molecular approaches for electrocatalytic hydrogen production in pure aqueous or aqueous-organic media, organized by the metal and ligand class employed.

## 2. Cobalt catalysts

Although there are no known biological systems that utilize cobalt for the catalytic reduction of protons to hydrogen, the

majority of reported small-molecule metal catalysts in aqueous media employ cobalt centers. We summarize the progress in molecular cobalt complexes for electrocatalytic hydrogen production in water, organized by ligand platforms.

### 2.1 Macrocyclic platforms

Among the earliest reported first-row transition metal catalysts for hydrogen generation in aqueous media were complexes based on azamacrocycles (Fig. 1). Fisher and Eisenberg reported a Co(II) tetraazamacrocyclic (1) that catalyzes the production of H<sub>2</sub> from protons with up to 80% Faradaic yield in 2 : 1 water-acetonitrile mixtures and pure water at  $-1.26$  V and  $-1.36$  V vs. SHE, respectively, on a Hg pool electrode.<sup>48</sup> Kellett and Spiro showed that water-soluble Co(II) complexes of *meso*-tetrakis(*N,N,N*-trimethylanilinium-4-yl)porphine chloride (2, CoTMAP), *meso*-tetrapyrro-4-ylporphine (3, CoTPyP), and *meso*-tetrakis(*N*-methylpyridinium-4-yl)porphine chloride (4, CoTMPyP) exhibit catalytic activity for proton reduction on a Hg electrode at  $-0.71$  V vs. SHE in 0.1 M trifluoroacetic acid (TFA) with over 90% Faradaic yield.<sup>49</sup> Proton reduction occurs at the Co(II)/Co(I) couple in DMSO solutions spiked with water and in neutral and acidic buffered solutions. More recently, bis(1,4,7-triazacyclodecane)cobalt(III) (5) has been reported to catalyze proton reduction at an onset potential of around  $-1.29$  V vs. SHE in Britton-Robinson universal buffers at pH 2 to pH 10 on a hanging drop Hg electrode.<sup>50</sup> Peters and co-workers established that a Co(II) tetraazamacrocyclic containing a pyridine donor (6) catalyzes hydrogen evolution at  $-0.69$  V vs. SHE with 92% Faradaic efficiency and a TON of 17 in pH 2.2 phosphate buffer on a glassy carbon plate electrode.<sup>51</sup> A feature observed prior to the onset

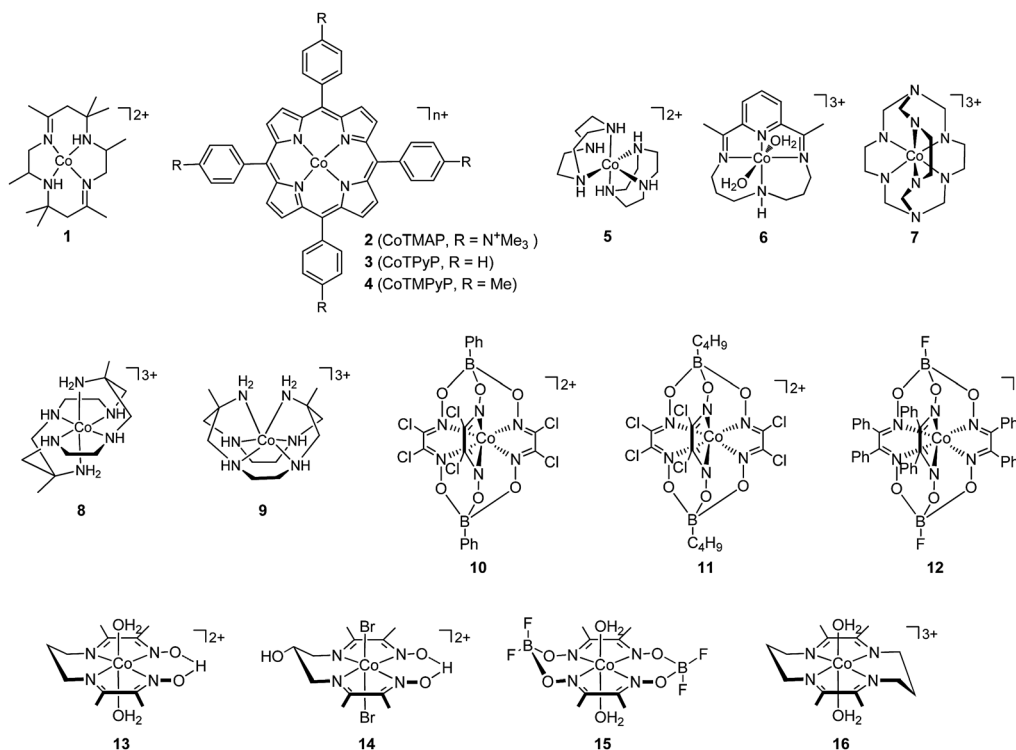


**Fig. 1** Structures of cobalt catalysts 1–16 with macrocyclic platforms.



of catalysis is assigned as a Co(II)/Co(I) couple, although there is some underlying catalytic activity at this process.

Cobalt chelates have also been studied for the catalytic reduction of protons to hydrogen. In an early study by Grätzel and co-workers, the use of  $[\text{Co}(\text{sepulchrate})]^{3+}$  (**7**) was demonstrated to afford catalytic  $\text{H}_2$  evolution. Controlled potential electrolysis at  $-0.46$  V vs. SHE in pH 4 phosphate buffer generates  $\text{H}_2$  at 55% Faradaic efficiency on a Hg pool electrode.<sup>52</sup> The complexes  $[\text{Co}(\text{trans-diammac})]^{2+}$  (**8**) and  $[\text{Co}(\text{cis-diammac})]^{2+}$  (**9**) can also catalyze proton reduction at  $-0.79$  V vs. SHE in pH 7 phosphate buffer on a Hg pool electrode.<sup>43</sup> Controlled potential electrolyses for both catalysts are carried out for up to 12 h and more than 10 equiv. of charge are passed. Interestingly, similar experiments are conducted using a reticulated vitreous carbon (RVC) electrode, but no catalytic activity is observed. Cyclic voltammograms of **8** and **9** show a reversible Co(II)/Co(I) process and an irreversible reductive process prior to water reduction. The current at the irreversible reduction varied linearly versus the scan rate, leading the authors to suggest that the active catalytic species was adsorbed on the Hg electrode. Complexes **8** and **9** are unique catalysts as the metal centers are coordinatively saturated and are unlikely to form Co hydride species. The authors hypothesize that upon a one-electron reduction, the Co(II) species is adsorbed on the surface of the electrode and generates a H atom on the surface of the electrode from the amine functionality of the ligand. This H atom then combines with another H atom to form hydrogen and the Co(II) species is reprotonated to regenerate the resting state.<sup>43</sup> A series of boron-capped tris(glyoximate) cobalt(II) complexes (**10** and **11**) was also reported to reduce the strong acid  $\text{HClO}_4$  to  $\text{H}_2$  in 1 : 1 water–acetonitrile mixtures at the first reductive event with an onset potential of around  $-0.19$  V vs. SHE.<sup>53</sup> Savéant and co-workers later established that **12**, a related tris(glyoximate) cobalt(II) first reported by Pantani and co-workers,<sup>54</sup> served as a molecular precursor for forming Co nanoparticles for hydrogen evolution in pH 7 phosphate buffer at  $-0.75$  V vs. SHE, with a 75–85% Faradaic yield on a glassy carbon foil electrode.<sup>55</sup> Since an initial report from Connolly and Espenson,<sup>56</sup> bis(dimethylglyoximate) cobalt(II) complexes have emerged as a class of proton reduction catalysts that have been studied extensively in organic media.<sup>36,57–59</sup> Peters and co-workers reported a series of bis(dimethylglyoximate) cobalt(II) catalysts (**13–16**) for proton reduction in acidic water (Fig. 1).<sup>51</sup> In pH 2.2 phosphate buffer on a glassy carbon electrode, cyclic voltammograms of both **13** and **14** show an irreversible reductive process that is consistent with catalytic proton reduction. Cyclic voltammograms of catalysts **15** and **16** both exhibit a feature that preceded the catalytic current and was assigned as a Co(II)/Co(I) couple. Controlled potential electrolyses of **13–16** at  $-0.69$  V vs. SHE are conducted over the course of 2 h and complex **13** is found to have the highest catalytic performance, generating  $\text{H}_2$  with 81% Faradaic yield and 23 turnovers. In a 24 h bulk electrolysis of **13**, the average catalytic current decreases relative to the initial 2 h electrolysis, but Faradaic efficiency is retained with a final cumulative yield of 86% (Fig. 2). To confirm the molecular nature of the catalyst, the glassy carbon electrode was removed from solution after a 2 h electrolysis and rinsed with water. Resubjecting the electrode to controlled potential electrolysis does not produce any catalytic activity (Fig. 2).

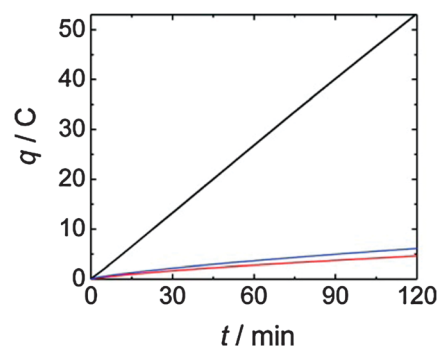


**Fig. 2** Controlled-potential electrolyses at  $-0.69$  V vs. SHE in the absence (red) and presence of **13** (black), in 0.1 M  $\text{NaClO}_4$  aqueous solution on a glassy carbon electrode. After a 2 h electrolysis, the electrode was rinsed with water and a controlled potential electrolysis under the same conditions in the absence of catalyst was conducted for 2 h (blue). Reprinted with the permission of American Chemical Society.<sup>51</sup>

## 2.2 Pyridine-based platforms

The versatile properties of pyridine as a neutral, strong-field ligand have inspired recent activity in using these donors for electrocatalytic reduction chemistry. To this end, our laboratory demonstrated that the Co(II) complex of the tetradentate bipyridine ligand PY4,  $[\text{Co}(\text{PY4OMe})]^{2+}$  (**17**), can reduce TFA to  $\text{H}_2$  in both acetonitrile and 1 : 1 water–acetonitrile solutions at ca.  $-0.76$  V vs. SHE (Table 1).<sup>60</sup> In addition, we presented a series of cobalt pentapyridine complexes of the type  $[\text{Co}(\text{RPY5Me}_2)]^{2+}$ , catalysts **18–20**, that are capable of reducing water at neutral pH (Fig. 3).<sup>61</sup> Cyclic voltammograms show that all three catalysts exhibit a pre-feature that lies on top of the onset of catalysis. In a controlled potential electrolysis at  $-1.30$  V vs. SHE in pH 7 phosphate buffer, complex **18** catalyzes hydrogen production at 99% Faradaic efficiency on a Hg pool electrode. There is no loss of activity after 60 h, and a TON of  $5.5 \times 10^4$  moles of  $\text{H}_2$  per mole of catalyst is measured. Of note, the electronic profile of the ligand is varied by changing the *para*-substituent on the axial pyridine. As expected for a molecular system, installation of a  $\text{CF}_3$  group, an electron-withdrawing substituent, significantly reduces the overpotential of catalytic proton reduction (Fig. 4). Conversely, installing an electron-donating  $\text{NMe}_2$  group increases the overpotential relative to the parent complex **18** (Fig. 4).

Bis(iminopyridine) cobalt(II) (**21**) was reported by Gray and Peters *et al.* to reduce protons in pH 2, 5, and 8 buffered water at  $-1.16$  V vs. SHE with Faradaic efficiencies of 75%, 87%, and 60%, respectively, on a Hg electrode.<sup>62</sup> Cyclic voltammograms in pH 7 phosphate buffer show two irreversible reductions prior to the onset of catalysis; however, the authors noted that current density from ligand reduction may contribute to the catalytic current density. Zhao and co-workers reported a pentacoordinate pyridyl-amine cobalt(II) complex with similarities to our PY5 systems,  $([\text{Co}(\text{DPA-Bpy})]^{2+}, \text{22})$ ,<sup>63</sup> for production of hydrogen from neutral pH water. In a cyclic voltammogram of **22** in pH 7 phosphate buffer, Co(III)/Co(II) and Co(II)/Co(I) couples are observed prior to the onset of catalysis at  $-1.2$  V vs. SHE. In a 1 h controlled potential electrolysis at  $-1.4$  V vs. SHE in pH 7 phosphate buffer, complex **22** is reported to catalyze hydrogen evolution with a

**Table 1** Electrochemical data for water-compatible cobalt catalysts for hydrogen evolution

Complex	Co(II)/Co(I) (V vs. SHE)	Applied potential (V vs. SHE) <sup>a</sup>	Faradaic efficiency (%)	TON (mol H <sub>2</sub> ) (mol cat) <sup>-1</sup>	TOF (mol H <sub>2</sub> ) (mol cat h) <sup>-1</sup>	Electrode	Conditions	Ref.
1	—	-1.26	—	—	—	Hg	2 : 1 H <sub>2</sub> O–MeCN	48
1	—	-1.36	<80	—	—	Hg	H <sub>2</sub> O	48
2	-0.42	-0.71	90	—	—	Hg	0.1 M TFA in H <sub>2</sub> O	49
3	-0.47	-0.71	90	—	—	Hg	0.1 M TFA in H <sub>2</sub> O	49
4	—	-0.71	90	—	—	Hg	0.1 M TFA in H <sub>2</sub> O	49
5	-1.29	-1.29	—	—	—	Hg	Britton–Robinson buffer pH 2–10	50
6	-0.53	-0.69	92	17	8.5 <sup>b</sup>	GC	pH 2.2 phosphate buffer	51
7	-0.3	-0.46	55	—	—	Hg	pH 4 phosphate buffer	52
8	—	-0.79	—	—	—	Hg	pH 7 phosphate buffer	43
9	—	-0.79	—	—	—	Hg	pH 7 phosphate buffer	43
10	-0.19	-0.19	—	—	—	GC	HClO <sub>4</sub> , 1 : 1 H <sub>2</sub> O–MeCN	53
11	-0.19	-0.19	—	—	—	GC	HClO <sub>4</sub> , 1 : 1 H <sub>2</sub> O–MeCN	53
12	—	-0.75	75–85	—	—	GC	pH 7 phosphate buffer	55
13	-0.52	-0.69	81	23	11.5 <sup>b</sup>	GC	pH 2.2 phosphate buffer	51
14	-0.52	-0.69	80	18	9 <sup>b</sup>	GC	pH 2.2 phosphate buffer	51
15	-0.39	-0.69	79	16	8 <sup>b</sup>	GC	pH 2.2 phosphate buffer	51
16	-0.53	-0.69	30	2	1 <sup>b</sup>	GC	pH 2.2 phosphate buffer	51
17	-0.76	-0.76	—	—	—	GC	TFA, 1 : 1 H <sub>2</sub> O–MeCN	60
18	-1.0	-1.3	>99	5.5 × 10 <sup>4</sup>	917 <sup>b</sup>	Hg	pH 7 phosphate buffer	61
19	-0.84	-1.3	—	—	—	Hg	pH 7 phosphate buffer	61
20	-1.12	-1.3	—	—	—	Hg	pH 7 phosphate buffer	61
21	-0.6	-1.16	75, 87, 60	—	7 × 10 <sup>6</sup> <sup>c</sup>	Hg	pH 2, 5, 8 aqueous buffer	62
22	-0.90	-1.4	99	300	300 <sup>b</sup>	Hg	pH 7 phosphate buffer	63
23	-0.63	-0.66	42	—	—	Hg	pH 6.5 phosphate buffer	52
24	—	-0.94	—	20	1.11 <sup>b</sup>	Hg	pH 5 phosphate buffer	42
25	-0.40	-0.77	>99	—	—	GC	TFA, 1 : 1 H <sub>2</sub> O–MeCN	64
26	-0.46	—	—	—	—	GC	TFA, 1 : 1 H <sub>2</sub> O–MeCN	64
27	-0.27	—	—	—	—	GC	TFA, 1 : 1 H <sub>2</sub> O–MeCN	64

<sup>a</sup> Catalytic onset potential where controlled potential electrolyses were not reported. <sup>b</sup> Calculated by dividing TON over the reported time of the electrolysis. <sup>c</sup> Calculated from  $j = nFC_p^0(Dk_{\text{app}}C_s^0)^{1/2}$ , where  $j$  is the current density,  $n$  is the number of electrons,  $F$  is Faraday's constant,  $D$  is the diffusion coefficient,  $k_{\text{app}}$  is the apparent rate constant, and  $C_p^0$  and  $C_s^0$  are the concentrations of the catalyst and the substrate, respectively.

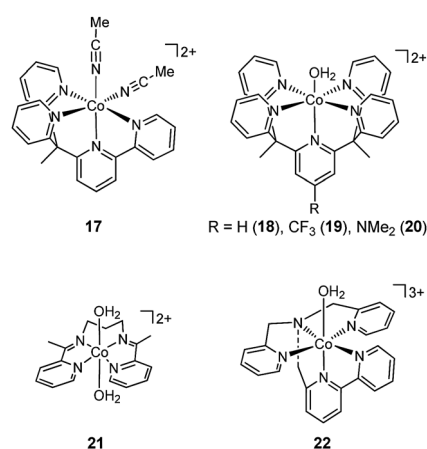


**Fig. 3** Structures of cobalt catalysts 17–22 featuring pyridine-based ligand platforms.

Faradaic yield of 99% and a TON of > 300 mol H<sub>2</sub> (mol cat)<sup>-1</sup> on a Hg pool electrode, with some decrease in catalytic activity after 3 h.

### 2.3 Other ligand platforms

Cyclopentadienyl cobalt complexes were amongst the earliest proton reduction catalysts examined in aqueous media (Fig. 5). Grätzel and co-workers reported that bis(carboxycyclopentadienyl) cobalt(III) ([Co(Cp-COOH)<sub>2</sub>]<sup>+</sup>, **23**) can serve as a water reduction

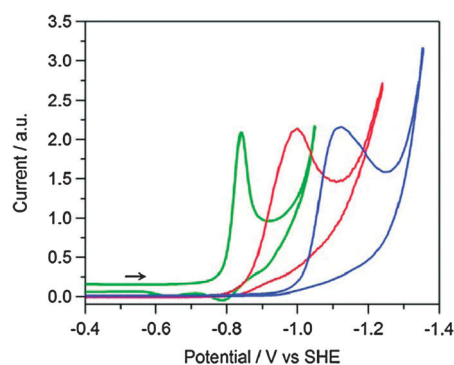


**Fig. 4** Cyclic voltammograms of **18** (red), **19** (green), and **20** (blue) in pH 7 phosphate buffer. Reprinted with the permission of American Chemical Society.<sup>61</sup>

catalyst at -0.66 V vs. SHE with a Faradaic efficiency of 42% in pH 6.5 phosphate buffer on a Hg pool electrode.<sup>52</sup> Koelle and Paul subsequently reported [CpCo(P(OMe)<sub>3</sub>)<sub>2</sub>]<sup>2+</sup> (**24**) as a catalyst for hydrogen evolution in water at pH 5 on a Hg pool electrode. A controlled potential electrolysis at -0.94 V vs. SHE for 18 h was conducted and a turnover number of 20 was determined.<sup>42</sup>

Eisenberg and Holland *et al.* recently reported that the bis(dithiolene) cobalt(II) complex (**25**) can reduce TFA to H<sub>2</sub> at -0.77 V vs. SHE in a 1 : 1 water–acetonitrile solution, with a Faradaic efficiency of >99% on a glassy carbon electrode.<sup>65</sup> Cyclic voltammograms of **25** show that the addition of TFA or tosic acid led to a current enhancement at the first reductive

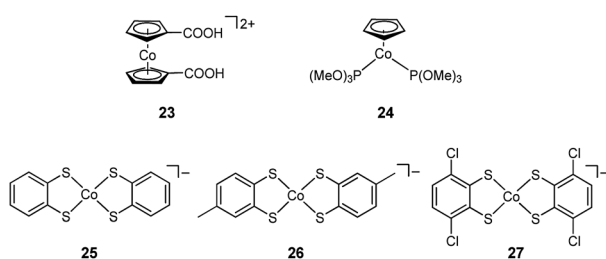


**Fig. 5** Structures of cobalt catalysts **23–27** with other ligand platforms.

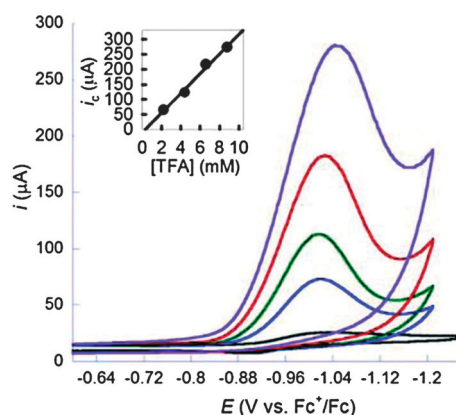


**Fig. 6** Cyclic voltammograms of 0.5 mM of **25** in a 0.1 M solution of  $\text{KNO}_3$  in 1 : 1 water–acetonitrile upon addition of 2.2 mM TFA (blue), 4.4 mM TFA (green), 6.6 mM TFA (red), and 8.8 mM TFA on a glassy carbon electrode. Inset: acid concentration dependence on current. Reprinted with the permission of American Chemical Society.<sup>65</sup>

process, formally a  $\text{Co(II)}/\text{Co(I)}$  couple (Fig. 6); however, due to the non-innocent nature of the ligand, protonation may occur either at the sulfur or at the metal. Interestingly, cyclic voltammograms of **25** in dry acetonitrile or *N,N*-dimethylformamide (DMF) lead to smaller current enhancements with the addition of acid. In a later study, the effects of electron-donating and electron-withdrawing groups on bis(benzenedithiolen)  $\text{Co(II)}$  complexes (**26** and **27**) were studied.<sup>64</sup> In particular, the installation of electron-withdrawing substituents causes a positive shift of the onset potential for catalytic hydrogen evolution. In a 1 : 1 water–acetonitrile solution on a glassy carbon electrode, catalyst **27**, which bears two  $\text{Cl}^-$  substituents, reduces TFA at the most positive catalytic potential of  $-0.71$  V vs. SHE, with a TON and TOF of  $6000 \text{ mol H}_2 (\text{mol cat})^{-1}$  and  $1400 \text{ h}^{-1}$ , respectively, after a 12 h bulk electrolysis.

#### 2.4 Observed trends in cobalt hydrogen electrocatalysts

The extensive body of research on Co catalysts offers some possible trends and mechanistic insights for future designs. Most importantly, the cyclic voltammograms of most of these systems exhibit a pre-feature prior to the onset of catalytic current that suggests the formation of a  $\text{Co(I)}$  species. Following Scheme 1, this  $\text{Co(I)}$  species can be protonated to form a  $\text{Co(III)-H}$ . Redox matching within this window, by either homolytic and/or heterolytic pathways, is critical to maintaining fast catalytic rates while minimizing overpotential. For complexes

that are chelated by non-innocent ligands, such as **7–12** and **21**, reduction and protonation of the ancillary ligand scaffold may play an important role in  $\text{H}_2$  evolution.

### 3. Nickel catalysts

Despite the prevalence of Ni–Fe hydrogenases found in the nature, relatively few nickel-based proton reduction catalysts that operate in aqueous media have been reported to date. A review on Ni–Fe hydrogenase mimics that function in pure organic media was recently published,<sup>66</sup> but activities of these enzyme models under aqueous conditions have not yet been reported. In an early study, Fisher and Eisenberg reported that Ni tetraazamacrocyclic (**28**) is a competent electrocatalyst for proton reduction at  $-1.46$  V vs. SHE in 2 : 1 water–acetonitrile mixtures on a Hg electrode (Fig. 7).<sup>48</sup> Sauvage and co-workers later reported that two Ni(II) complexes supported by 1,4,8,11-tetraazacyclotetradecane ( $[\text{Ni}(\text{cyclam})]^{2+}$ , **29**) and its bis-macrocyclic analog ( $[\text{Ni}_2(\text{biscyclam})]^{4+}$ , **30**) show catalytic activity toward proton reduction in neutral water on a Hg pool electrode.<sup>68</sup> Controlled potential electrolysis at  $-1.26$  V vs. SHE reveals that **30** is a better hydrogen evolution catalyst than **29** and can achieve TONs reaching 100, presumably due to the close proximity of two Ni centers and the ability to form Ni hydride intermediates.

Electrocatalytic hydrogen generation by Ni bis(phosphine) complexes has also been heavily investigated in recent years, most notably in elegant work from the Dubois laboratories.<sup>35,47,69,70</sup> A large body of research has focused on installing pendant amines as biomimetic proton relays for the reduction of organic acids at the Ni(II)/Ni(I) couple in acetonitrile. Recently, a family of Ni bis(phosphine) complexes  $[\text{Ni}(\text{PPh}_2\text{NC}_6\text{H}_4\text{X}_2)_2]^{2+}$ , **31–36**, was reported to have enhanced electrocatalytic activity when water was added to acidic acetonitrile solutions (Table 2).<sup>71</sup> Catalyst **33**, where  $\text{X} = \text{CH}_2\text{P}(\text{O})(\text{OEt}_2)_2$ , exhibits a TOF of  $500 \text{ s}^{-1}$  at an overpotential of 320 mV in pure acetonitrile on a glassy carbon electrode; addition of water leads to a TOF of  $1850 \text{ s}^{-1}$  at an overpotential of 370 mV. A new variant of  $[\text{Ni}(\text{P}_2\text{N}_2)_2]^{2+}$ , catalyst **37**, has also been found to reduce protons in acidic ionic liquid–water solutions with a TOF of  $>4 \times 10^{-4} \text{ s}^{-1}$  at an overpotential of 400 mV.<sup>72</sup> A similar trend was discovered for  $[\text{Ni}(\text{PPh}_2\text{NPh})_2]^{2+}$  (**38**), where TOFs of  $33000 \text{ s}^{-1}$  and  $106000 \text{ s}^{-1}$

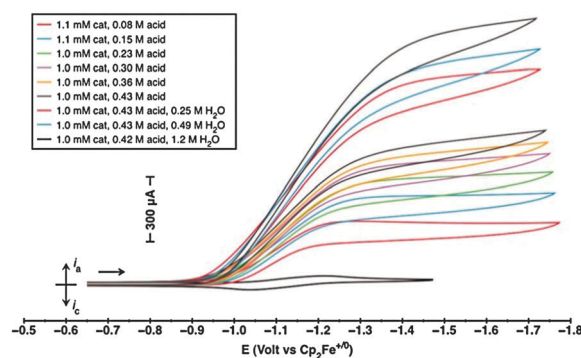


**Fig. 7** Cyclic voltammograms of **38** in the presence of increasing concentrations of DMF : H<sub>2</sub>O, and followed by the addition of water in an acetonitrile solution on a glassy carbon electrode. Reprinted with the permission of American Association for the Advancement of Science.<sup>67</sup>

**Table 2** Electrochemical data for water-compatible nickel, iron, and molybdenum catalysts for hydrogen evolution

Complex	$M^{n+}/M^{n-1}$ (V vs. SHE)	Applied potential <sup>a</sup> (V vs. SHE)	Faradaic efficiency (%)	TON (mol H <sub>2</sub> (mol cat) <sup>-1</sup> )	TOF (mol H <sub>2</sub> (mol cat h) <sup>-1</sup> )	Electrode	Conditions	Ref.
28	—	-1.46	—	—	—	Hg	2 : 1 H <sub>2</sub> O–MeCN	48
29	-1.34	-1.26	—	—	—	Hg	0.1 M NaClO <sub>4</sub> in H <sub>2</sub> O	68
30	-1.18	-1.26	—	—	—	Hg	0.1 M NaClO <sub>4</sub> in H <sub>2</sub> O	68
31	-0.1	-0.18 <sup>b</sup>	—	—	$4.3 \times 10^5$ <sup>c</sup>	GC	DMF : HOTf, 0.27 M H <sub>2</sub> O in MeCN	71
32	-0.14	-0.17 <sup>b</sup>	—	—	$3.7 \times 10^6$ <sup>c</sup>	GC	DMF : HOTf, 0.27 M H <sub>2</sub> O in MeCN	71
33	-0.19	-0.25 <sup>b</sup>	—	—	$6.7 \times 10^6$ <sup>c</sup>	GC	DMF : HOTf, 0.55 M H <sub>2</sub> O in MeCN	71
34	-0.18	-0.20 <sup>b</sup>	—	—	$2.6 \times 10^6$ <sup>c</sup>	GC	DMF : HOTf, 0.034 M H <sub>2</sub> O in MeCN	71
35	-0.19	-0.24 <sup>b</sup>	—	—	$2.8 \times 10^6$ <sup>c</sup>	GC	DMF : HOTf, 0.05 M H <sub>2</sub> O in MeCN	71
36	-0.14	-0.21 <sup>b</sup>	94 (at -0.26 V)	—	$1.7 \times 10^6$ <sup>c</sup>	GC	DMF : HOTf, 0.08 M H <sub>2</sub> O in MeCN	71
37	-0.62 <sup>d</sup>	-1.0 <sup>d</sup>	92	13	$4.3 \times 10^4$ <sup>e</sup>	GC–RVC	X = 0.72 H <sub>2</sub> O in [(DBF)H]NTf <sub>2</sub>	72
38	-0.49	-0.49	—	—	$1.1 \times 10^5$ <sup>e</sup>	GC	DMF : HOTf, 1.2 M H <sub>2</sub> O in MeCN	67
39	-0.13	-0.5	—	—	—	GC	TsOH, 0.2 M NaClO <sub>4</sub> in H <sub>2</sub> O	73
40	—	-1.1	95	—	—	RVC	0.1 M KCl–HCl in H <sub>2</sub> O (pH 1)	74
41	-1.53	-1.7	—	—	—	GC	HOAc, 1 : 3 H <sub>2</sub> O–MeCN	75
42	-1.38	-1.7	—	—	—	GC	HOAc, 1 : 3 H <sub>2</sub> O–MeCN	75
43	-1.7 <sup>e</sup>	-1.63 <sup>e</sup>	—	—	—	GC	HOAc, 1 : 3 H <sub>2</sub> O–MeCN	76
44	-1.8 <sup>e</sup>	-1.63 <sup>e</sup>	—	—	—	GC	HOAc, 1 : 3 H <sub>2</sub> O–MeCN	76
45	—	-1.26	—	—	—	GC	MeCN spiked with H <sub>2</sub> O	77
46	—	-1.27	—	—	—	GC	MeCN spiked with H <sub>2</sub> O	77
47	—	-0.66	100	52	52 <sup>g</sup>	Hg	HOAc, pH 3 water with 10 mM sodium dodecyl sulfate	78
48	-1.06 <sup>f</sup>	-1.4	> 99	$6.1 \times 10^5$	8500	Hg	pH 7 phosphate buffer	79
49	-0.53 <sup>f</sup>	-0.96	> 99	$1.9 \times 10^7$	$1.9 \times 10^7$ <sup>h</sup>	Hg	pH 3 acetate buffer	46

<sup>a</sup> Catalytic onset potential where controlled potential electrolyses were not reported. <sup>b</sup> Back-calculated using the Felton method<sup>31</sup> ( $E_{\text{HA}^\circ} = -0.518$ ) as only overpotentials were reported. <sup>c</sup> Calculated from eqn (4). <sup>d</sup> Potential was referenced to Fc/Fc<sup>+</sup>. <sup>e</sup> Potentials were referenced to Ag/AgNO<sub>3</sub>. <sup>f</sup> Mo(III)/Mo(II) reduction potential. <sup>g</sup> Calculated by dividing TON over the reported time of the electrolysis. <sup>h</sup> Calculated based on the surface coverage of the catalyst on the Hg pool.

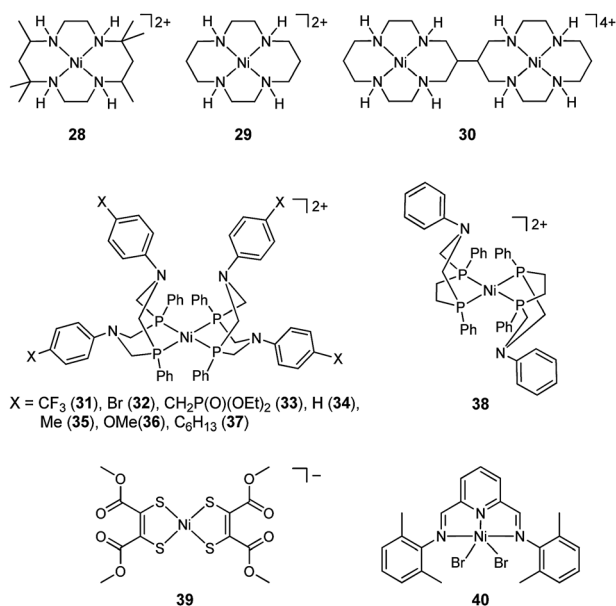
were achieved in pure acetonitrile and 1.2 M of water in acetonitrile, respectively, at -0.49 V vs. SHE (Fig. 7).<sup>67</sup> This remarkable rise in catalytic activity was attributed to the ability of water to enhance the rate of formation of the *endo* isomer, which allowed a second N–H stabilization. Other derivatives of Ni bis(phosphines) have been examined for proton reduction activity under water-compatible conditions.<sup>80,81</sup>

Similar to its Co(II) dithiolene analogues,<sup>64,65</sup> Ni(II) dithiolene (**39**) was reported by Sarkar and co-workers to catalyze the

reduction of tosic acid to H<sub>2</sub> in 0.2 M NaClO<sub>4</sub> in water at -0.5 V vs. SHE on a glassy carbon electrode coated with **39**.<sup>73</sup> Crabtree, Brudvig, and Batista *et al.* described Ni(II) complexes supported by pyridinediimine (**40**) for reducing water at pH 1 at -1.1 V vs. SHE on a vitreous carbon electrode at 95% Faradaic efficiency (Fig. 8).<sup>74</sup>

#### 4. Iron catalysts

The majority of Fe catalysts for hydrogen generation have targeted functional Fe–Fe hydrogenase mimics that operate in acidic organic media.<sup>5,82–87</sup> To increase the aqueous compatibility of these types of compounds, water-soluble 1,3,5-triaza-7-phosphaadamantane (PTA) has been employed as ligands in diiron scaffolds. Darensbourg and co-workers reported two diiron thiolate clusters (**41** and **42**) for electrocatalytic reduction of acetic acid to H<sub>2</sub> in acetonitrile and water–acetonitrile solutions at *ca.* -1.7 V vs. SHE on a glassy carbon electrode.<sup>75</sup> Although controlled potential electrolyses in mixed water–acetonitrile solutions are not reported, cyclic voltammograms of **41** and **42** with acetic acid in water–acetonitrile mixtures lead to positive shifts of all redox potentials and higher catalytic current relative to the redox potentials in pure acetonitrile solutions. Sun and co-workers reported similar findings for analogous diiron azadithiolates (**43** and **44**).<sup>76</sup> Another method introduced by Sun *et al.* to make diiron clusters more water-compatible is to attach a carboxylate side chain for hydrogen bonding.<sup>77</sup> Cyclic voltammograms of **45** and **46** in acetonitrile solutions spiked with aliquots of water lead to modest current enhancements at the onset potential of -0.86 V vs. SHE, highlighting the importance of the carboxylic group. Recently, a hydrophobic diiron cluster (**47**) is used as a proton reduction catalyst

**Fig. 8** Structures of nickel catalysts **25–40**.



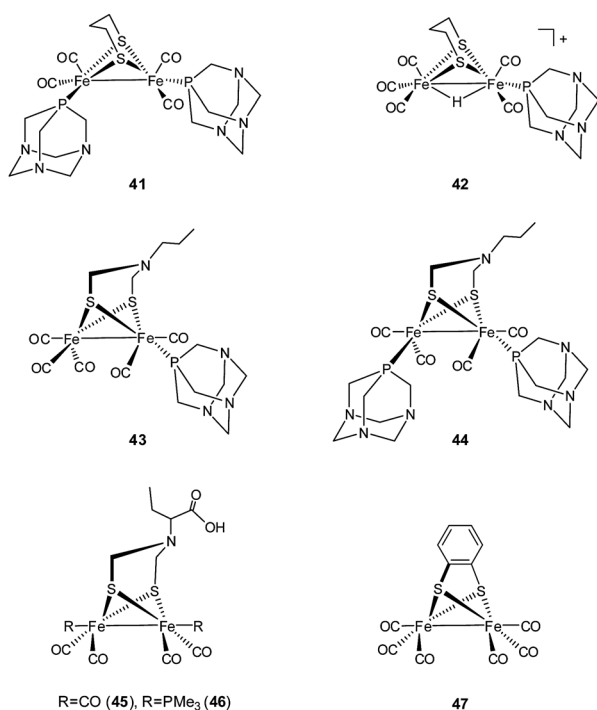


Fig. 9 Structures of iron catalysts 41–47.

at  $-0.66$  V vs. SHE in pH 3 aqueous micellar solutions and generates hydrogen at Faradaic efficiency (Fig. 9).<sup>78</sup>

## 5. Molybdenum catalysts

Our laboratories have explored high-valent molybdenum complexes as a unique family of molecular motifs for catalytic hydrogen generation. Initial studies focused on metal–oxo species as reductive catalysts, inspired by the elegant water activation work of Blum and Milstein,<sup>88</sup> Yoon and Tyler,<sup>89</sup> and Bercaw and Parkin<sup>90</sup> as well as Toste's original hydrosilylation methodologies using oxorhenium catalysts.<sup>91</sup> In particular, we reasoned that this motif would provide greater catalytic stability in aqueous solutions, as any potential off-pathway reactions would ultimately funnel back to the metal–oxo species and thus return to productive catalytic cycles, akin to Nocera's "self-healing" catalysts for water oxidation.<sup>3,92,93</sup> Thus, the key challenge for this approach is developing appropriate supporting ligands for metal–oxo complexes that can favor sufficient reductive chemistry.

Along these lines, we recently established that the Mo(IV)–oxo complex  $[(PY5Me_2)MoO]^{2+}$  (**48**), upon electrochemical reduction, can catalytically convert water to hydrogen at a potential of  $-1.4$  V vs. SHE in pH 7 phosphate buffer on a Hg pool electrode.<sup>79</sup> This catalytic system maintains full activity for at least 71 h and operates at 100% Faradaic efficiency. Lower-bound values for the TOF and TON are  $8500$  h<sup>-1</sup> and  $6.1 \times 10^5$  moles of H<sub>2</sub> per mole of catalyst, respectively. Moreover, this catalytic system can operate in seawater with similar activity, showing that the reactivity of the MoPY5 motif is tolerant of aqueous impurities and that the ionic strength of seawater is a sufficient medium to maintain electrocatalysis. Further theoretical and experimental studies suggest that three reductive events are necessary

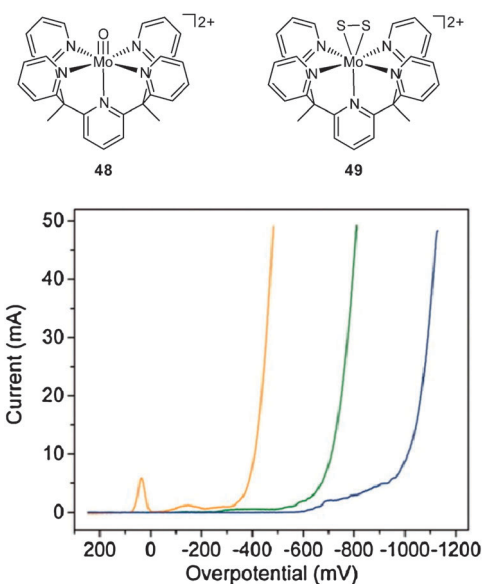


Fig. 10 Structures of molybdenum catalysts **48** and **49** and cyclic voltammograms in the absence (blue) and presence of **48** (green), **49** (orange) in pH 3 acetate buffer on a Hg pool electrode. Reprinted with the permission of American Association for the Advancement of Science.<sup>46</sup>

to reach the catalytically active species for hydrogen generation and establish that the catalyst can operate under soluble, diffusion-limited conditions on alternative electrode materials and solvents.<sup>45,94</sup> Taken together with select Co macrocycles, these studies on  $[(PY5Me_2)MoO]^{2+}$  (**48**) provide a rare example of an electrocatalyst that has been evaluated both in aqueous and organic solutions.

Inspired by emerging studies on molybdenum–sulfide materials as low-cost platinum replacements for catalytic proton reduction,<sup>23–27</sup> we recently reported that electrochemical reduction of the molecular complex  $[(PY5Me_2)MoS_2]^{2+}$  (**49**) can also catalytically reduce water under acidic aqueous conditions on a Hg pool electrode (Fig. 10).<sup>46</sup> Complex **49** represents a rare coordination compound with a side-on bound S<sub>2</sub><sup>2-</sup> on the Mo(IV) that mimics the reactive edge sites of the two-dimensional solid MoS<sub>2</sub>. A 23 h controlled potential electrolysis of **49** at an overpotential of 780 mV in pH 3 acetate buffer generated hydrogen at 100% Faradaic efficiency, with a lower-limit TON value calculated from bulk solution of  $3.5 \times 10^3$  moles of H<sub>2</sub> per mole catalyst and an upper limit of  $1.9 \times 10^7$  moles of H<sub>2</sub> per mole catalyst assuming a constant monolayer on the electrode. The catalytic activity of **48** and **49** highlights the potential of using high-valent metal complexes as well as metal–ligand multiple bonded species for reductive catalysis in water. More generally, this MoS<sub>2</sub> work has implications for the design of structural and functional molecular mimics of extended solid materials, in much the same way that bioinorganic chemists distill the structure and reactivity of enzymes and other complex biological macromolecules by modelling discrete metal active sites.

## 6. Surface-attached molecular catalysts

An alternative approach to water-soluble molecular catalysts for aqueous compatibility is to tether these systems to solid electroactive supports.<sup>11,12</sup> In addition to potential gains in

stability and selectivity due to isolation of active sites, the use of high-surface area electrodes may significantly decrease the catalyst loading and reduce the cost of production. We highlight a selection of examples here to give the reader a flavor of the field. In one example, glassy carbon electrodes modified with polyoxometallates (POMs)  $[\text{Co}_6(\text{H}_2\text{O})_{30}(\text{Co}_9\text{Cl}_2(\text{OH})_3(\text{H}_2\text{O})_9(\beta\text{-SiW}_8\text{O}_{31})_3)]^{5-}$  (**50**) and  $[(\text{Co}_3(\text{B-}\beta\text{-SiW}_9\text{O}_{33}(\text{OH}))(\text{B-}\beta\text{-SiW}_8\text{O}_{29}(\text{OH}))_2)]^{22-}$  in Vulcan-XC72/Nafion and poly(4-vinylpyridine) are used to reduce protons in acidic water.<sup>95</sup> Cyclic voltammograms of **50** in 0.5 M  $\text{H}_2\text{SO}_4$  show catalytic current at *ca.*  $-0.2$  V *vs.* SHE after cycling the potential from 0 to  $-0.6$  V *vs.* SHE for 35 min at  $100$   $\text{mV s}^{-1}$ . Pantani and co-workers reported that glassy carbon electrodes modified with Co and Ni diglyoximate complexes embedded in Nafion can also catalyze proton reduction in 1 M  $\text{H}_2\text{SO}_4$  aqueous solutions, with Co diglyoximate outperforming its Ni analogues.<sup>96</sup> A more recent report by Berben and Peters showed that catalyst **15** can be adsorbed onto a glassy carbon electrode in the presence of tosic acid in acetonitrile during a controlled potential electrolysis held at  $-0.34$  V *vs.* SHE.<sup>97</sup> The modified electrode is used for catalytic proton reduction in pH 4 acetate solutions and generates hydrogen with 75% Faradaic efficiency at an overpotential of 400 mV. A TON of  $5 \times 10^6$  was observed, and the current remains stable for 16 h.

Other Co tetraazamacrocycles have also been attached to electrode surfaces. Co porphyrin complexes adsorbed onto glassy carbon electrodes show catalytic hydrogen generation, but the stability of the attachment is poor.<sup>98</sup>  $[\text{Co}(\text{tetraphenylporphyrin})]^{2+}$  incorporated into a Nafion membrane on a Pt electrode exhibits greater catalytic activity than the activity of both the catalyst alone and a bare Pt electrode.<sup>99</sup> A TON of  $70 \text{ h}^{-1}$  is achieved at  $-0.49$  V *vs.* SHE in pH 1 phosphate solution. Co phthalocyanine complexes embedded into poly(4-vinylpyridine-co-styrene) film on a graphite electrode can catalyze proton reduction at  $-0.69$  V *vs.* SHE in pH 1 phosphate buffer with a TON of  $2 \times 10^5 \text{ h}^{-1}$ .<sup>100</sup> Artero, Fontecave, and co-workers showed that Dubois-type Ni bis(phosphine) complexes can be covalently attached through an amide functionality to multi-walled carbon nanotubes and deposited by dropcasting with Nafion onto a glassy carbon electrode to facilitate hydrogen evolution in water (Fig. 11).<sup>101</sup> The immobilized catalyst can reduce protons in  $\text{H}_2\text{SO}_4$  aqueous solutions at

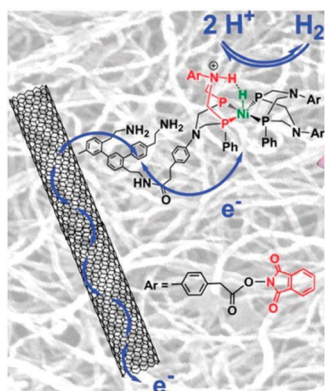


**Fig. 11** Schematic representation of the bio-inspired  $\text{H}_2$ -evolving nickel catalyst grafted on a carbon nanotube. Reprinted with the permission of American Association for the Advancement of Science.<sup>101</sup>

$-20$  mV *vs.* SHE and with over 100 000 turnovers. Pyrene attachments to carbon nanotubes show similar reactivity.<sup>102</sup> Finally, Chorkendorff and co-workers have reported that incomplete cubane-type  $\text{Mo}_3\text{S}_4$  molecules adsorbed onto a graphite electrode can act as an efficient catalyst system for hydrogen generation, with an onset potential of  $-0.2$  V *vs.* SHE in 0.5 M  $\text{H}_2\text{SO}_4$  aqueous solutions.<sup>103</sup> Photoelectrochemical studies further support that the  $\text{Mo}_3\text{S}_4$  clusters are catalytically active for proton reduction in acidic water.<sup>104</sup> Here,  $\text{Mo}_3\text{S}_4$  clusters are adsorbed onto p-doped Si pillars and found to catalyze proton reduction at  $-0.15$  V *vs.* SHE (an overpotential of 400 mV when the photovoltage is added) in 0.1 M  $\text{HClO}_4$  aqueous solution under photoillumination of  $> 650$  nm, with a TOF of  $950 \text{ s}^{-1}$ .

## 7. Concluding remarks and future prospects

We have highlighted a number of classes of molecular platforms for catalytic electrochemical reduction of protons to hydrogen, focusing on systems that utilize cheap and earth-abundant metal centers and exhibit aqueous compatibility. These molecular systems provide a valuable complement to emerging bulk solid-state materials used for proton reduction,<sup>3,23–27</sup> as they offer benefits for mechanistic study and tuning through rational ligand design. We emphasize that the use of water as both a solvent and a substrate has advantages for maintaining high substrate concentration and minimizing environmental impact from organic additives and by-products, and that aqueous-compatible molecular catalysis is therefore an attractive area to continue exploring in the context of green and sustainable chemistry.

Numerous opportunities await the next-generation of molecular systems for catalytic hydrogen production from aqueous media. The most important fundamental challenge is to continue to discover and identify novel molecular motifs for proton reduction, which can serve as lead compounds for new materials synthesis or help elucidate the principles by which complex solid-state or biological systems operate. Basic science, and in particular inorganic coordination chemistry, can drive innovation toward these goals.

On the practical side, improved long-term stability and/or regeneration of molecular species is a key issue. Grafting well-defined catalytic units onto high surface-area electrodes has the potential to increase their lifetime and catalytic performance by site isolation, as well as to control the density of these small-footprint active sites. Integration of water reduction and oxidation half-reactions into a single artificial device is necessary for efficient water-splitting cycles, and these opposing reactions must operate under compatible conditions without the risk of premature recombination of protons and electrons. In this context, the application of proton exchange membranes<sup>105</sup> to resolve this issue remains an open question for investigation. Finally, solar energy offers the most sustainable option as an energy input, and many fundamental issues in integration are important venues for study. Matching the energies of photosensitizer excited states to catalyst redox potentials, as well as optimizing distance and orientation between light-harvesting and catalyst components are some of the critical questions to address. Molecular approaches to these outstanding challenges, in addition to the catalytic applications described in this review, will continue to play an important role in the development of sustainable energy technologies.

## Acknowledgements

Our work in sustainable energy catalysis is supported by DOE/LBNL Grant 403801 (C.J.C.) and the Joint Center for Artificial Photosynthesis, a DOE Energy Innovation Hub, supported through the Office of Science of the U.S. Department of Energy under award DE-SC0004993 (J.R.L.). V.S.T. thanks the National Science Foundation for a Graduate Research Fellowship. C.J.C. is an Investigator with the Howard Hughes Medical Institute.

## Notes and references

- N. S. Lewis and D. G. Nocera, *Proc. Natl. Acad. Sci. U. S. A.*, 2006, **103**, 15729–15735.
- A. J. Esswein and D. G. Nocera, *Chem. Rev.*, 2007, **107**, 4022–4047.
- T. R. Cook, D. K. Dogutan, S. Y. Reece, Y. Surendranath, T. S. Teets and D. G. Nocera, *Chem. Rev.*, 2010, **110**, 6474–6502.
- M. Frey, *ChemBioChem*, 2002, **3**, 153–160.
- D. J. Evans and C. J. Pickett, *Chem. Soc. Rev.*, 2003, **32**, 268–275.
- F. A. Armstrong, *Curr. Opin. Chem. Biol.*, 2004, **8**, 133–140.
- K. A. Vincent, A. Parkin and F. A. Armstrong, *Chem. Rev.*, 2007, **107**, 4366–4413.
- A. M. Kluwer, R. Kapre, F. Hartl, M. Lutz, A. L. Spek, A. M. Brouwer, P. W. N. M. van Leeuwen and J. N. H. Reek, *Proc. Natl. Acad. Sci. U. S. A.*, 2009, **106**, 10460–10465.
- E. Reisner, *Eur. J. Inorg. Chem.*, 2011, 1005–1016.
- P. A. Ash and K. A. Vincent, *Chem. Commun.*, 2012, **48**, 1400–1409.
- T. W. Woolerton, S. Sheard, Y. S. Chaudhary and F. A. Armstrong, *Energy Environ. Sci.*, 2012, **5**, 7470.
- F. A. Armstrong, *Curr. Opin. Chem. Biol.*, 2005, **9**, 110–117.
- S. K. Ibrahim, X. Liu, C. d. Tard and C. J. Pickett, *Chem. Commun.*, 2007, 1535.
- C. M. Thomas, O. Rüdiger, T. Liu, C. E. Carson, M. B. Hall and M. Y. Darensbourg, *Organometallics*, 2007, **26**, 3976–3984.
- A. Le Goff, V. Artero, R. Metayé, F. Moggia, B. Jousset, M. Razavet, P. D. Tran, S. Palacin and M. Fontecave, *Int. J. Hydrogen Energy*, 2010, **35**, 10790–10796.
- J. O. M. Bockris and B. E. Conway, *Trans. Faraday Soc.*, 1949, **45**, 989–999.
- H. Ezaki, M. Morinaga and S. Watanabe, *Electrochim. Acta*, 1993, **38**, 557–564.
- B. C. H. Steele and A. Heinzl, *Nature*, 2001, **414**, 345–352.
- M. K. Debe, *Nature*, 2012, **486**, 43–51.
- O. Savadogo and H. Lavoie, *Int. J. Hydrogen Energy*, 1992, **17**, 473–477.
- O. Savadogo, *J. Electrochem. Soc.*, 1992, **139**, 1082–1087.
- O. Savadogo, F. Carrier and E. Forget, *Int. J. Hydrogen Energy*, 1994, **19**, 429–435.
- B. Hinnemann, P. G. Moses, J. Bonde, K. P. Jørgensen, J. H. Nielsen, S. Horch, I. Chorkendorff and J. K. Nørskov, *J. Am. Chem. Soc.*, 2005, **127**, 5308–5309.
- T. F. Jaramillo, K. P. Jørgensen, J. Bonde, J. H. Nielsen, S. Horch and I. Chorkendorff, *Science*, 2007, **317**, 100–102.
- Y. Li, H. Wang, L. Xie, Y. Liang, G. Hong and H. Dai, *J. Am. Chem. Soc.*, 2011, **133**, 7296–7299.
- D. Merki, S. Fierro, H. Vruble and X. Hu, *Chem. Sci.*, 2011, **2**, 1262–1267.
- D. Merki, H. Vruble, L. Rovelli, S. Fierro and X. Hu, *Chem. Sci.*, 2011, **3**, 2515–2525.
- V. Artero, M. Chavarot-Kerlidou and M. Fontecave, *Angew. Chem., Int. Ed.*, 2011, **50**, 7238–7266.
- P. Du and R. Eisenberg, *Energy Environ. Sci.*, 2012, **5**, 6012–6021.
- M. Wang, L. Chen and L. Sun, *Energy Environ. Sci.*, 2012, **5**, 6763–6778.
- G. A. N. Felton, R. S. Glass, D. L. Lichtenberger and D. H. Evans, *Inorg. Chem.*, 2006, **45**, 9181–9184.
- A. Kütt, I. Leito, I. Kaljurand, L. Sooväli, V. M. Vlasov, L. M. Yagupolskii and I. A. Koppel, *J. Org. Chem.*, 2006, **71**, 2829–2838.
- K. Kaupmees, I. Kaljurand and I. Leito, *J. Phys. Chem. A*, 2010, **114**, 11788–11793.
- V. Fourmond, P.-A. Jacques, M. Fontecave and V. Artero, *Inorg. Chem.*, 2010, **49**, 10338–10347.
- D. H. Pool and D. L. DuBois, *J. Organomet. Chem.*, 2009, **694**, 2858–2865.
- C. Baffert, V. Artero and M. Fontecave, *Inorg. Chem.*, 2007, **46**, 1817–1824.
- J. L. Dempsey, J. R. Winkler and H. B. Gray, *J. Am. Chem. Soc.*, 2010, **132**, 16774–16776.
- B. H. Solis and S. Hammes-Schiffer, *Inorg. Chem.*, 2011, **50**, 11252–11262.
- B. H. Solis and S. Hammes-Schiffer, *J. Am. Chem. Soc.*, 2011, **133**, 19036–19039.
- J. T. Muckerman and E. Fujita, *Chem. Commun.*, 2011, **47**, 12456–12458.
- L. E. Fernandez, S. Horvath and S. Hammes-Schiffer, *J. Phys. Chem. C*, 2011, **116**, 3171–3180.
- U. Koelle and S. Paul, *Inorg. Chem.*, 1986, **25**, 2689–2694.
- P. V. Bernhardt and L. A. Jones, *Inorg. Chem.*, 1999, **38**, 5086–5090.
- A. M. Appel, D. L. DuBois and M. Rakowski DuBois, *J. Am. Chem. Soc.*, 2005, **127**, 12717–12726.
- E. J. Sundstrom, X. Yang, V. S. Thoi, H. I. Karunadasa, C. J. Chang, J. R. Long and M. Head-Gordon, *J. Am. Chem. Soc.*, 2012, **134**, 5233–5242.
- H. I. Karunadasa, E. Montalvo, Y. Sun, M. Majda, J. R. Long and C. J. Chang, *Science*, 2012, **335**, 698–702.
- M. Rakowski DuBois and D. L. DuBois, *Chem. Soc. Rev.*, 2009, **38**, 62–72.
- B. J. Fisher and R. Eisenberg, *J. Am. Chem. Soc.*, 1980, **102**, 7361–7363.
- R. M. Kellett and T. G. Spiro, *Inorg. Chem.*, 1985, **24**, 2373–2377.
- R. Abdel-Hamid, H. M. El-Sagher, A. M. Abdel-Mawgoud and A. Nafady, *Polyhedron*, 1998, **17**, 4535–4541.
- C. C. L. McCrory, C. Uyeda and J. C. Peters, *J. Am. Chem. Soc.*, 2012, **134**, 3164–3170.
- V. Houlding, T. Geiger, U. Kölle and M. Grätzel, *J. Chem. Soc., Chem. Commun.*, 1982, 681.
- Y. Z. Voloshin, A. V. Dolganov, O. A. Varzatskii and Y. N. Bubnov, *Chem. Commun.*, 2011, **47**, 7737.
- O. Pantani, S. Naskar, R. Guillot, P. Millet, E. Anxolabéhère-Mallart and A. Aukauloo, *Angew. Chem., Int. Ed.*, 2008, **47**, 9948–9950.
- E. Anxolabéhère-Mallart, C. Costentin, M. Fournier, S. Nowak, M. Robert and J.-M. Savéant, *J. Am. Chem. Soc.*, 2012, **134**, 6104–6107.
- P. Connolly and J. H. Espenson, *Inorg. Chem.*, 1986, **25**, 2684–2688.
- X. Hu, B. M. Cossairt, B. S. Brunshwig, N. S. Lewis and J. C. Peters, *Chem. Commun.*, 2005, 4723–4725.
- X. Hu, B. S. Brunshwig and J. C. Peters, *J. Am. Chem. Soc.*, 2007, **129**, 8988–8998.
- J. L. Dempsey, B. S. Brunshwig, J. R. Winkler and H. B. Gray, *Acc. Chem. Res.*, 2009, **42**, 1995–2004.
- J. P. Bigi, T. E. Hanna, W. H. Harman, A. Chang and C. J. Chang, *Chem. Commun.*, 2010, **46**, 958–960.
- Y. Sun, J. P. Bigi, N. A. Piro, M. L. Tang, J. R. Long and C. J. Chang, *J. Am. Chem. Soc.*, 2011, **133**, 9212–9215.
- B. D. Stubbart, J. C. Peters and H. B. Gray, *J. Am. Chem. Soc.*, 2011, **133**, 18070–18073.
- W. M. Singh, T. Baine, S. Kudo, S. Tian, X. A. N. Ma, H. Zhou, N. J. DeYonker, T. C. Pham, J. C. Bollinger, D. L. Baker, B. Yan, C. E. Webster and X. Zhao, *Angew. Chem., Int. Ed.*, 2012, **51**, 5941–5944.
- W. R. McNamara, Z. Han, C.-J. Yin, W. W. Brennessel, P. L. Holland and R. Eisenberg, *Proc. Natl. Acad. Sci. U. S. A.*, 2012, DOI: 10.1073/pnas.1120757109.
- W. R. McNamara, Z. Han, P. J. Alperin, W. W. Brennessel, P. L. Holland and R. Eisenberg, *J. Am. Chem. Soc.*, 2011, **133**, 15368–15371.
- S. Canaguier, V. Artero and M. Fontecave, *Dalton Trans.*, 2008, 315.
- M. L. Helm, M. P. Stewart, R. M. Bullock, M. R. DuBois and D. L. DuBois, *Science*, 2011, **333**, 863–866.

- 68 J. P. Collin, A. Jouaiti and J. P. Sauvage, *Inorg. Chem.*, 1988, **27**, 1986–1990.
- 69 A. D. Wilson, R. H. Newell, M. J. McNevin, J. T. Muckerman, M. Rakowski DuBois and D. L. DuBois, *J. Am. Chem. Soc.*, 2005, **128**, 358–366.
- 70 M. Rakowski Dubois and D. L. Dubois, *Acc. Chem. Res.*, 2009, **42**, 1974–1982.
- 71 U. J. Kilgore, J. A. S. Roberts, D. H. Pool, A. M. Appel, M. P. Stewart, M. R. DuBois, W. G. Dougherty, W. S. Kassel, R. M. Bullock and D. L. DuBois, *J. Am. Chem. Soc.*, 2011, **133**, 5861–5872.
- 72 D. H. Pool, M. P. Stewart, M. O'Hagan, W. J. Shaw, J. A. S. Roberts, R. M. Bullock and D. L. DuBois, *Proc. Natl. Acad. Sci. U. S. A.*, DOI: 10.1073/pnas.1120208109.
- 73 A. Begum, G. Moula and S. Sarkar, *Chem.–Eur. J.*, 2010, **16**, 12324–12327.
- 74 O. R. Luca, S. J. Konezny, J. D. Blakemore, D. M. Colosi, S. Saha, G. W. Brudvig, V. S. Batista and R. H. Crabtree, *New J. Chem.*, 2012, **36**, 1149–1152.
- 75 R. Mejia-Rodriguez, D. Chong, J. H. Reibenspies, M. P. Soriaga and M. Y. Darensbourg, *J. Am. Chem. Soc.*, 2004, **126**, 12004–12014.
- 76 Z. Wang, J. Liu, C. He, S. Jiang, B. Åkermark and L. Sun, *Inorg. Chim. Acta*, 2007, **360**, 2411–2419.
- 77 W. Gao, J. Sun, T. Åkermark, M. Li, L. Eriksson, L. Sun and B. Åkermark, *Chem.–Eur. J.*, 2010, **16**, 2537–2546.
- 78 F. Quentel, G. Passard and F. Gloaguen, *Energy Environ. Sci.*, 2012, **5**, 7757–7761.
- 79 H. I. Karunadasa, C. J. Chang and J. R. Long, *Nature*, 2010, **464**, 1329–1333.
- 80 A. Jain, S. Lense, J. C. Linehan, S. Raugei, H. Cho, D. L. DuBois and W. J. Shaw, *Inorg. Chem.*, 2011, **50**, 4073–4085.
- 81 S. Wiese, U. J. Kilgore, D. L. DuBois and R. M. Bullock, *ACS Catal.*, 2012, **2**, 720–727.
- 82 F. d. r. Gloaguen, J. D. Lawrence and T. B. Rauchfuss, *J. Am. Chem. Soc.*, 2001, **123**, 9476–9477.
- 83 M. Y. Darensbourg, E. J. Lyon, X. Zhao and I. P. Georgakaki, *Proc. Natl. Acad. Sci. U. S. A.*, 2003, **100**, 3683–3688.
- 84 L. Sun, B. Åkermark and S. Ott, *Coord. Chem. Rev.*, 2005, **249**, 1653–1663.
- 85 C. Tard, X. Liu, S. K. Ibrahim, M. Bruschi, L. D. Gioia, S. C. Davies, X. Yang, L.-S. Wang, G. Sawers and C. J. Pickett, *Nature*, 2005, **433**, 610–613.
- 86 G. A. N. Felton, A. K. Vannucci, J. Chen, L. T. Lockett, N. Okumura, B. J. Petro, U. I. Zakai, D. H. Evans, R. S. Glass and D. L. Lichtenberger, *J. Am. Chem. Soc.*, 2007, **129**, 12521–12530.
- 87 F. Gloaguen and T. B. Rauchfuss, *Chem. Soc. Rev.*, 2009, **38**, 100–108.
- 88 O. Blum and D. Milstein, *J. Am. Chem. Soc.*, 2002, **124**, 11456–11467.
- 89 M. Yoon and D. R. Tyler, *Chem. Commun.*, 1997, 639–670.
- 90 G. Parkin and J. E. Bercaw, *J. Am. Chem. Soc.*, 1989, **111**, 391–393.
- 91 J. J. Kennedy-Smith, K. A. Nolin, H. P. Gunterman and F. D. Toste, *J. Am. Chem. Soc.*, 2003, **125**, 4056–4057.
- 92 M. W. Kanan and D. G. Nocera, *Science*, 2008, **321**, 1072–1075.
- 93 D. G. Nocera, *Acc. Chem. Res.*, 2012, **45**, 767–776.
- 94 V. S. Thoi, H. I. Karunadasa, Y. Surendranath, J. R. Long and C. J. Chang, *Energy Environ. Sci.*, 2012, **5**, 7762–7770.
- 95 B. Keita, U. Kortz, L. R. B. Holze, S. Brown and L. Nadjo, *Langmuir*, 2007, **23**, 9531–9534.
- 96 O. Pantani, E. Anxolabéhère-Mallart, A. Aukauloo and P. Millet, *Electrochem. Commun.*, 2007, **9**, 54–58.
- 97 L. A. Berben and J. C. Peters, *Chem. Commun.*, 2010, **46**, 398–400.
- 98 R. M. Kellett and T. G. Spiro, *Inorg. Chem.*, 1985, **24**, 2378–2382.
- 99 T. Abe, F. Taguchi, H. Imai, F. Zhao, J. Zhang and M. Kaneko, *Polym. Adv. Technol.*, 1998, **9**, 559–562.
- 100 F. Zhao, J. Zhang, T. Abe, D. Wöhrle and M. Kaneko, *J. Mol. Catal. A: Chem.*, 1999, **145**, 245–256.
- 101 A. Le Goff, V. Artero, B. Jusselme, P. D. Tran, N. Guillet, R. Métayé, A. Fihri, S. Palacin and M. Fontecave, *Science*, 2009, **326**, 1384–1387.
- 102 P. D. Tran, A. Le Goff, J. Heidkamp, B. Jusselme, N. Guillet, S. Palacin, H. Dau, M. Fontecave and V. Artero, *Angew. Chem., Int. Ed.*, 2011, **50**, 1371–1374.
- 103 T. F. Jaramillo, J. Bonde, J. Zhang, B.-L. Ooi, K. Andersson, J. Ulstrup and I. Chorkendorff, *J. Phys. Chem. C*, 2008, **112**, 17492–17498.
- 104 Y. Hou, B. L. Abrams, P. C. K. Vesborg, M. E. Björketun, K. Herbst, L. Bech, A. M. Setti, C. D. Damsgaard, T. Pedersen, O. Hansen, J. Rossmesl, S. Dahl, J. K. Nørskov and I. Chorkendorff, *Nat. Mater.*, 2011, **10**, 434–438.
- 105 M. T. Dinh Nguyen, A. Ranjbari, L. Catala, F. Brisset, P. Millet and A. Aukauloo, *Coord. Chem. Rev.*, 2012, **256**, 2435–2444.